

# Revisiting the Bragg reflector to illustrate some modern developments in optics

S. A. R. Horsley

*Electromagnetic and Acoustic Materials Group,  
Department of Physics and Astronomy,  
University of Exeter, Stocker Road, Exeter, EX4 4QL, UK\**

J.-H. Wu

*College of Physics, Jilin University, Changchun 130012, P. R. China*

M. Artoni

*European Laboratory for Nonlinear Spectroscopy, Sesto Fiorentino, Italy and  
Department of Engineering and Information Technology  
CNR-IDASC Sensor Lab, Brescia University, Brescia, Italy*

G. C. La Rocca

*Scuola Normale Superiore and CNISM, Pisa, Italy*

(Dated: December 2, 2024)

## Abstract

A dielectric composed of a sequence of similar thin layers of alternating refractive index is well known to make a good mirror when radiation close to normal incidence has a wavelength within the medium of around four times the layer thickness. Such a device—often termed the *Bragg reflector*—is usually introduced to students within the first years of an undergraduate degree, and often in isolation from other parts of the course. Here we show that the basic physics of wave propagation through a stratified medium can be used to illustrate some more modern developments in optics as well as quantum physics; from transfer matrix techniques, to the optical properties of cold trapped atoms, optomechanical cooling, and a simple example of a system exhibiting an appreciable level of optical non-reciprocity.

## I. INTRODUCTION

To paraphrase Griffiths<sup>3</sup>, wave motion can be divided into at least three kinds. These are travelling waves (continuous spectrum); bound states (discrete spectrum); and waves within a periodic medium (continuous spectrum with forbidden regions). There are a variety of ways in which the third of this number can be introduced. Perhaps the most obvious route is through condensed matter physics, where the atomic lattice provides a ubiquitous example of a periodic medium (see e.g.<sup>5-7</sup>). To all intents and purposes such a system has an infinite number of periods, where Bloch's theorem approaches exactitude.

Yet it is instructive to observe the emergence of Bloch's theorem as the number of periods of the system is increased. Indeed the motion of waves in a one dimensional periodic, layered medium can be solved exactly for any number of layers<sup>1-4</sup>. A neat example where the onset of a band gap may be observed can be found in the optics of the Bragg reflector<sup>1</sup>: an optical medium composed of layers of two kinds of material with differing refractive indices. Possibly the most striking lesson one learns through studying an arbitrary number of layers is how quickly the results of Bloch's theorem become applicable as the number of layers is increased from unity.

Not only is the Bragg reflector useful for discussing the emergence of Bloch's theorem, but it also unveils some subtleties of propagation in a periodic medium. Dispersion and dissipation significantly alter the picture, and dissipation in particular can cause a breakdown of the distinction between allowed and forbidden bands of frequency. In this work we derive the optical properties of the Bragg reflector through an application of the transfer matrix formalism<sup>8</sup>, and the results are applied to the discussion of the optical properties of a lattice of cold trapped atoms<sup>9</sup>, where both dispersion and dissipation are significant at the frequencies of interest. As we shall see, the picture becomes quite different when these effects are included.

Further to this we show that the Bragg reflector can be used to introduce the principles of two phenomena of current interest: optomechanical cooling<sup>10</sup>; and optical non-reciprocity<sup>11,12</sup>. In both cases the high frequency sensitivity close to a band edge significantly couples the optical response to the centre of mass motion of the reflector, and thereby provides a simple example system where such motional effects can be evident.

## II. STRATIFIED MEDIA AND TRANSFER MATRICES

In many cases, knowledge of the transfer matrix reduces the problem of solving a linear wave equation in an inhomogeneous medium to that of multiplying together  $2 \times 2$  matrices<sup>1,8,13</sup>. The wave could be electromagnetic, quantum mechanical, vibrational, fluid mechanical, and so on—so long as the dynamics of the wave-propagation is linear. In the case of electromagnetic waves in periodic, layered, planar media the formalism is particularly neat. It therefore seems appropriate to introduce the Bragg reflector via the transfer matrix formalism.

The system under consideration is illustrated in figure 1, where we have a dielectric ( $\mu = \mu_0$ ) medium composed of  $N$  homogeneous layers, each with a different value of  $\epsilon = \epsilon_0 n^2$ , immersed in background medium of  $\epsilon_c = \epsilon_0 n_c^2$ . For arbitrary angles of incidence the propagation of waves through the medium depends on the polarization, and in anisotropic or moving media, the transfer matrix can become a  $4 \times 4$  object, which significantly complicates matters<sup>14–16</sup>. In our case it is sufficient to assume normal incidence onto a medium composed of isotropic layers, where the behaviour of the two polarizations is degenerate, and the transfer matrix is a  $2 \times 2$  object.

For a fixed frequency,  $\omega$  the solution to the wave equation within each slice of the medium (illustrated in figure 1) is a plane wave, with the spatial dependence of the field being proportional to  $\exp(\pm i k_x x)$  ( $k_x = n(\omega)\omega/c$  is different in each slice). With this in mind, the electric field at every point in space is written as a sum of two parts; a *right* moving part,  $e^{(+)}(x)$ , and a *left* moving part,  $e^{(-)}(x)$ , with the understanding that the full field is the sum of the two,  $\mathbf{E}(x) = \hat{\chi}^{(+)} e^{(+)}(x) + \hat{\chi}^{(-)} e^{(-)}(x)$ , where  $\hat{\chi}^{(\pm)}$  are the unit vectors denoting the polarization of the waves. The  $2 \times 2$  matrix,  $\mathbf{M}$ , that relates these two parts of the field across the whole structure is the *transfer matrix*, and the components of  $\mathbf{M}$  determine the reflection and transmission coefficients of the medium. The only question is how to determine  $\mathbf{M}$ .

In this case we calculate the transfer matrix associated with getting from the background medium,  $n_c$ , on the left of figure 1, through the  $N$  layers, to then again emerge into the background medium,  $n_c$ , on the right. There are only two kinds of things that happen to the light during propagation: it crosses boundaries, and it moves through homogeneous media. The full transfer matrix is thus broken up into two kinds of component matrices, an

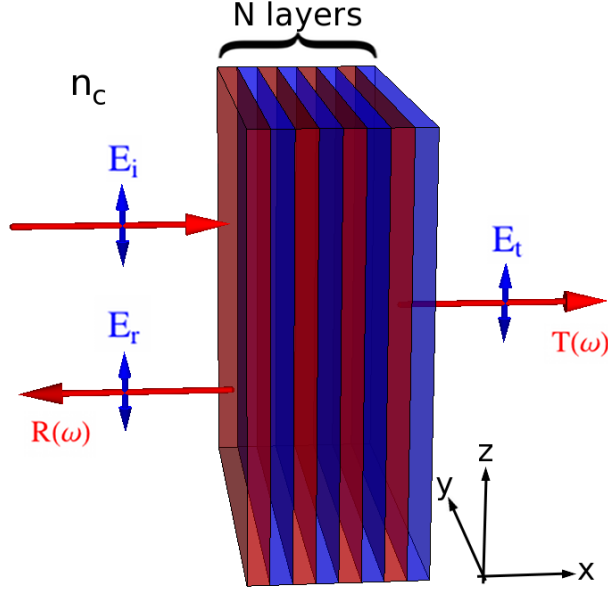


FIG. 1: An  $N$  layer structure is surrounded by a medium with a real refractive index  $n_c$ .

In the rest frame of the medium, we imagine linearly polarized light of frequency,  $\omega$  is incident from the left with electric field amplitude,  $\mathbf{E}_i$ , some of which is reflected as  $\mathbf{E}_r$  (reflectivity,  $R(\omega)$ ), and some of which is transmitted as  $\mathbf{E}_t$  (transmittivity,  $T(\omega)$ ).

“interface” matrix,  $\mathbf{W}$ , that relates the field across a boundary, and a “translation” matrix,  $\mathbf{X}$ , that relates the components of the field after propagation through a homogeneous region. In both cases superscripts are introduced into the notation to indicate the media being referred to. The operation of these two matrices is illustrated in figure 2.

The matrix,  $\mathbf{W}$  can be found through applying the condition of continuity of the tangential  $\mathbf{E}$  and  $\mathbf{H}$  fields<sup>17</sup>. For normal incidence and non-magnetic media ( $\mu \sim \mu_0$ ), e.g.  $\mathbf{E} = E_a \hat{\mathbf{z}}$  and  $\mathbf{H} = (i/\mu_0\omega)\hat{\mathbf{y}}\partial E_a/\partial x$ , this amounts to the continuity of the electric field and its first derivative across the boundary. Applying these conditions on the electric field across an interface between index  $n_a$  and  $n_b$  (see 2a) at  $x = \text{const.}$ , we have

$$e_a^{(+)} + e_a^{(-)} = e_b^{(+)} + e_b^{(-)}, \quad (1)$$

and,

$$n_a [e_a^{(+)} - e_a^{(-)}] = n_b [e_b^{(+)} - e_b^{(-)}]. \quad (2)$$

where we have used the relation,  $\partial e^{(\pm)}/\partial x = \pm ik_x e^{(\pm)}$  to obtain (2). The above two equations

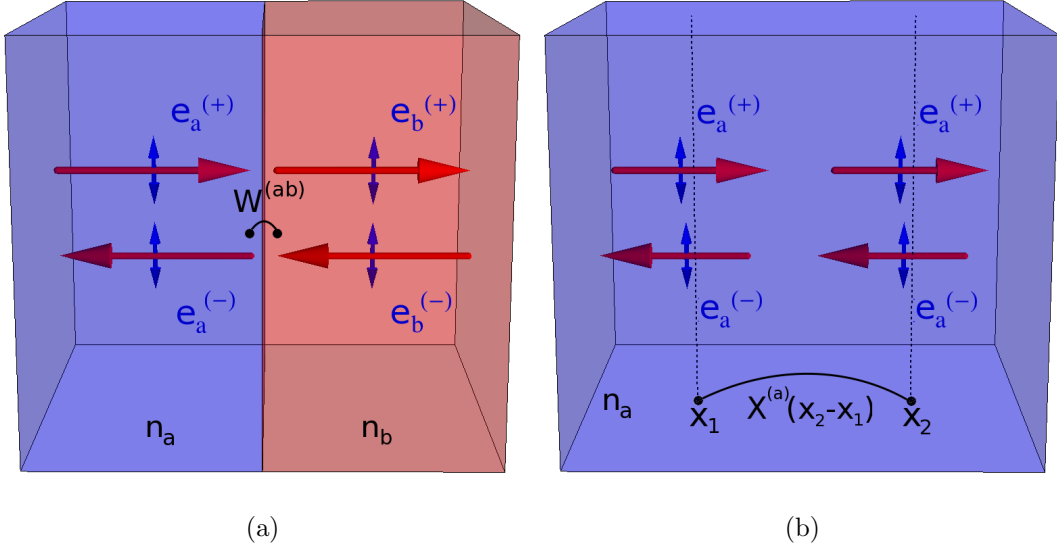


FIG. 2: We consider the total transfer matrix,  $M$ , to relate the electric field amplitude of a light wave passing from the left to the right of the multilayer stack in figure 1. In general  $M$  can be decomposed into a product of  $2N + 1$  component matrices that are each of two kinds denoted by  $\mathbf{W}$  and  $\mathbf{X}$ , the actions of which are illustrated in subfigures (a) and (b).

In (a), the “interface” matrix,  $\mathbf{W}^{(ab)}$ , relates the electric field on the immediate left of a boundary (here with index  $n_a$ ), to the field on the immediate right ( $n_b$ ). Meanwhile, in (b) the “translation” matrix  $\mathbf{X}^{(a)}(x_2 - x_1)$  relates the electric fields between two points in a homogeneous medium ( $x_1$  and  $x_2$ ), that we here take to have index  $n_a$ .

may be cast in matrix form,

$$\begin{pmatrix} 1 & 1 \\ n_a & -n_a \end{pmatrix} \begin{pmatrix} e_a^{(+)} \\ e_a^{(-)} \end{pmatrix} = \begin{pmatrix} 1 & 1 \\ n_b & -n_b \end{pmatrix} \begin{pmatrix} e_b^{(+)} \\ e_b^{(-)} \end{pmatrix}$$

and through inverting the  $2 \times 2$  matrix on the left, the matrix associated with crossing the boundary  $n_a \rightarrow n_b$  is obtained,

$$\begin{pmatrix} e_b^{(+)} \\ e_b^{(-)} \end{pmatrix} = \frac{1}{2} \begin{pmatrix} 1 + n_a/n_b & 1 - n_a/n_b \\ 1 - n_a/n_b & 1 + n_a/n_b \end{pmatrix} \begin{pmatrix} e_a^{(+)} \\ e_a^{(-)} \end{pmatrix} \equiv \mathbf{W}^{(ab)} \begin{pmatrix} e_a^{(+)} \\ e_a^{(-)} \end{pmatrix}. \quad (3)$$

The matrix in (3) defines the general relation between the electric fields across a boundary between two media with different refractive indices. Note that when  $n_a = n_b$ ,  $\mathbf{W}^{(ab)} = \mathbf{1}_2$ , and also that the matrix is transitive,  $\mathbf{W}^{(bc)} \cdot \mathbf{W}^{(ab)} = \mathbf{W}^{(ac)}$ .

The operation of the matrix,  $\mathbf{X}$  associated with propagation of the field through a distance,  $x_2 - x_1$  within a homogeneous medium is illustrated in figure 2b and is simply obtained through multiplying  $e^{(+)}$  and  $e^{(-)}$  by the phase factor,  $\exp(\pm ik_x(x_2 - x_1))$ , e.g. for a medium of index  $n_a$ ,

$$\begin{pmatrix} e_a^{(+)}(x_2) \\ e_a^{(-)}(x_2) \end{pmatrix} = \begin{pmatrix} e^{ik_a(x_2-x_1)} & 0 \\ 0 & e^{-ik_a(x_2-x_1)} \end{pmatrix} \begin{pmatrix} e_a^{(+)}(x_1) \\ e_a^{(-)}(x_1) \end{pmatrix} \equiv \mathbf{X}^{(a)}(x_2 - x_1) \begin{pmatrix} e_a^{(+)}(x_1) \\ e_a^{(-)}(x_1) \end{pmatrix}. \quad (4)$$

The matrices, (3) and (4) can be used to study light propagation in *generic* stratified media. In the limit of infinitesimally thin slices they can also be used to treat continuously inhomogeneous media<sup>1</sup>. From here on we consider media with periodically varying layers of finite thickness.

### III. THE BRAGG REFLECTOR: A 1D PHOTONIC CRYSTAL

The transfer matrix approach discussed above is now applied to a stratified medium composed of a *periodic* sequence of identical unit cells (figure 3), each cell containing two isotropic dielectric layers having different complex refractive indices, and thicknesses: such a structure is often termed a Bragg reflector. Rayleigh<sup>18</sup>, and Bragg<sup>19</sup> were among the first to begin to develop an understanding of wave propagation in periodic media, but it is only relatively recently that it has been possible to manufacture three dimensional structures with inhomogeneities on the scale of an optical wavelength<sup>20,21</sup>. This, along with theoretical work illustrating interesting properties such as inhibited spontaneous emission<sup>22,23</sup>, photon localization<sup>24</sup>, and negative refraction<sup>25</sup>, has seen these systems garner the separate general designation “photonic crystals”. Consequently, in modern terms the Bragg reflector can be recognised as an ordered one dimensional photonic crystal, despite the fact that the optics of thin films significantly predates this modern work<sup>26,27</sup>. The periodic variation in the optical response of such media leads to Bragg scattering of light in much the same way as for electrons in crystalline solids<sup>2,3</sup> (c.f. sect. III A), and this generally leads to the appearance of photonic band gaps with a very steep frequency variation of the reflectivity and transmissivity profiles around the band-edge.

The unit-cell of our periodic dielectric multilayer is sketched in figure 3. The relation of the electric field at the beginning of cell  $i$  to that at the beginning of cell  $(i + 1)$  can be envisaged as a sequence of  $\mathbf{W}$  and  $\mathbf{X}$  operations, as in figure 2. The unit-cell is identified

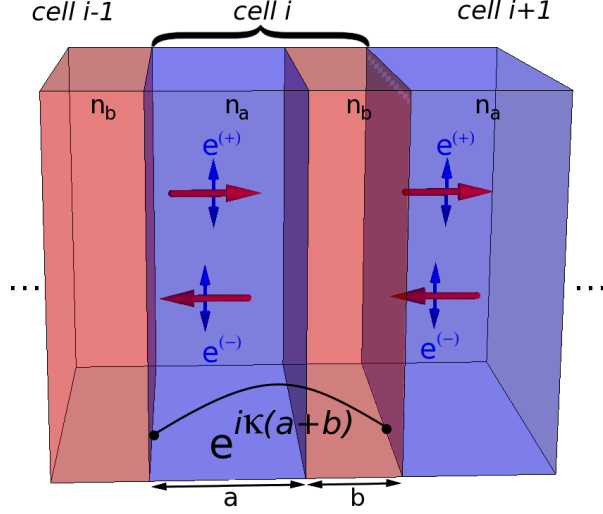


FIG. 3: The unit cell of a Bragg reflector (c.f. figure 1). This is chosen so that it *begins* and *ends* infinitesimally to the right of the  $n_b \rightarrow n_a$  boundary. The relationship between the fields in cell  $i$  and  $i + 1$  is determined by  $\mathcal{M}_1$ . The relationship between the field just to the right of the  $n_b \rightarrow n_a$  boundary in one cell, and just to the right of the same boundary  $N$  unit cells later is instead determined by  $\mathcal{M}_N$  (cf. (8)). For a truly infinite periodic structure, the difference in the field across a unit cell is a phase factor  $e^{i\kappa(a+b)}$ , determined by the Bloch wave-vector,  $\kappa$  and the crystal periodicity  $(a + b)$ .

as starting and finishing within a medium of index  $n_a$ , which is equivalent to the following sequence of matrices,

$$\begin{aligned} \mathcal{M}_1 &= \mathbf{W}^{(ba)} \cdot \mathbf{X}^{(b)}(b) \cdot \mathbf{W}^{(ab)} \cdot \mathbf{X}^{(a)}(a) \\ &= \begin{pmatrix} [\cos(k_b b) + i\alpha_{ab} \sin(k_b b)] e^{ik_a a} & -i\beta_{ab} \sin(k_b b) e^{-ik_a a} \\ i\beta_{ab} \sin(k_b b) e^{ik_a a} & [\cos(k_b b) - i\alpha_{ab} \sin(k_b b)] e^{-ik_a a} \end{pmatrix}, \end{aligned} \quad (5)$$

where,  $k_{a,b} = n_{a,b} \omega / c$ ,  $\alpha_{ab} = (n_a^2 + n_b^2) / (2n_a n_b)$ , and  $\beta_{ab} = (n_a^2 - n_b^2) / (2n_a n_b)$  (recall  $n_a$  and  $n_b$  are complex functions of  $\omega$ ).

The matrix associated with the passage of light through  $N$  identical unit cells is the  $N$ th power of the above unit-cell matrix,  $\mathcal{M}_N = \mathcal{M}_1^N$ . Given that  $\mathcal{M}_1$  is a  $2 \times 2$  matrix, we can write  $\mathcal{M}_N$  in a particularly elegant form involving Chebyshev polynomials of the second

kind<sup>1-3</sup>. To see how this is done, consider the square of a general  $2 \times 2$  matrix,  $\mathbf{A}$ ,

$$\begin{aligned} \mathbf{A}^2 &= \begin{pmatrix} a_{11} & a_{12} \\ a_{21} & a_{22} \end{pmatrix} \begin{pmatrix} a_{11} & a_{12} \\ a_{21} & a_{22} \end{pmatrix} = \begin{pmatrix} a_{11}^2 + a_{12}a_{21} & a_{12}(a_{11} + a_{22}) \\ a_{21}(a_{11} + a_{22}) & a_{22}^2 + a_{12}a_{21} \end{pmatrix} \\ &= \text{Tr}[\mathbf{A}]\mathbf{A} - \det[\mathbf{A}]\mathbb{1}_2 \end{aligned} \quad (6)$$

Having obtained (6) it is clear that it must be possible to write the  $N$ th power of  $\mathbf{A}$  in the form  $\mathbf{A}^N = a_N\mathbf{A} + b_N\mathbb{1}_2$ . Multiplying this proposed form on the left by  $\mathbf{A}$ , and applying (6), we obtain the recurrence relations,  $a_{N+1} = a_N\text{Tr}[\mathbf{A}] + b_N$ , and  $b_{N+1} = -a_N\det[\mathbf{A}]$ , which is equivalent to,  $a_{N+1} = \text{Tr}[\mathbf{A}]a_N - \det[\mathbf{A}]a_{N-1}$ . Meanwhile, the Chebyshev polynomials satisfy a very similar recursion relation<sup>28</sup>,

$$U_{N+1}(z) = 2zU_N(z) - U_{N-1}(z) \quad (7)$$

this relation holding for both the Chebyshev polynomials of the first,  $T_N(z)$ , and second,  $U_N(z)$  kinds<sup>28</sup>. The difference between  $T_N(z)$  and  $U_N(z)$  is in the choice of initial values:  $\{T_0 = 1, T_1 = z\}$ , and  $\{U_0 = 1, U_1 = 2z\}$ . If  $\det[\mathbf{A}] = 1$ , then the coefficients,  $a_N$  satisfy (7), and we find that  $\mathbf{A}^N = U_{N-1}(z)\mathbf{A} - U_{N-2}(z)\mathbb{1}_2$ , with  $z = \text{Tr}[\mathbf{A}]/2$ . We must choose the Chebyshev polynomial of the second kind because we must obtain (6) when  $N = 2$ . We assume  $\det[\mathbf{M}_N] = 1$ , which for our purposes is always the case<sup>16,29</sup> (see (34) below).

The  $N$ -cell matrix thus takes the form,

$$\mathbf{M}_N = U_{N-1}(z)\mathbf{M}_1 - U_{N-2}(z)\mathbb{1}_2, \quad (8)$$

where,

$$z = \frac{1}{2}\text{Tr}(\mathbf{M}_1) = \cos(k_b b) \cos(k_a a) - \alpha_{ba} \sin(k_b b) \sin(k_a a). \quad (9)$$

with  $\mathbf{M}_1$  given by (5), and where the Chebyshev polynomials may be computed from their relation to the trigonometric functions<sup>28</sup>:  $U_N(z) = \sin[(N+1)\arccos(z)]/\sqrt{1-z^2}$ .

The transfer matrix,  $\mathbf{M}$ , for the situation illustrated in figure 1 is  $\mathbf{M}_N$  sandwiched between two matrices associated with light passing from the background index,  $n_c$ , into the multilayer,

$$\mathbf{M} = \begin{pmatrix} m_{11} & m_{12} \\ m_{21} & m_{22} \end{pmatrix} = \mathbf{W}^{(ac)} \cdot \mathbf{M}_N \cdot \mathbf{W}^{(ca)}, \quad (10)$$

where we apply  $\mathbf{W}^{(bc)} \cdot \mathbf{W}^{(ab)} = \mathbf{W}^{(ac)}$ . The relationship between the electric field amplitudes on the left and right of figure 1 is finally given by  $\mathbf{e}_R = \mathbf{M} \cdot \mathbf{e}_L$ , where  $\mathbf{e}_{L,R}$  here refers to the two row vector composed of the left and right going parts of the field.

Reflection from, and transmission through the system can now be calculated: light of amplitude  $E_0$  is incident from the left, and the transfer matrix equation reduces to,

$$\begin{pmatrix} E_0 t_+ \\ 0 \end{pmatrix} = \begin{pmatrix} m_{11} & m_{12} \\ m_{21} & m_{22} \end{pmatrix} \begin{pmatrix} E_0 \\ E_0 r_+ \end{pmatrix}$$

from which follows expressions for the reflectivity and and transmissivity,

$$\begin{aligned} T_+ &\equiv |t_+|^2 = \left| \frac{\det[\mathbf{M}]}{m_{22}} \right|^2 \\ R_+ &\equiv |r_+|^2 = \left| \frac{m_{21}}{m_{22}} \right|^2 \end{aligned} \tag{11}$$

assuming that  $n_c$  is real. Similarly, for incidence from the right we have,

$$\begin{pmatrix} E_0 r_- \\ E_0 \end{pmatrix} = \begin{pmatrix} m_{11} & m_{12} \\ m_{21} & m_{22} \end{pmatrix} \begin{pmatrix} 0 \\ E_0 t_- \end{pmatrix}$$

which gives,

$$\begin{aligned} T_- &\equiv |t_-|^2 = \left| \frac{1}{m_{22}} \right|^2 \\ R_- &\equiv |r_-|^2 = \left| \frac{m_{12}}{m_{22}} \right|^2 \end{aligned} \tag{12}$$

Consequently (11) and (12) are not equal in general. This is not too surprising. It is straightforward to imagine multilayer systems where identical reflectivity for incidence from the left and the right would not be expected. One example would be a highly reflective surface backed by a thick layer of strongly absorbing material: incidence onto the front surface would yield a reflectivity close to unity, while incidence onto the reverse would yield a much lower value. The situation is not so clear in the case of the transmission coefficient, as one requires  $\det[\mathbf{M}] \neq 1$  in order for  $T_+ \neq T_-$ : such a system would be optically non-reciprocal<sup>11,17</sup>, which is a non-trivial property in electromagnetism. We shall return to this issue in section IV C.

For our specific system the transfer matrix is (10). Inserting (3), (5), and (8) into (10) gives the explicit expressions for the reflectivity and transmissivity of this system. The

elements of the transfer matrix are found to be

$$\begin{aligned}
m_{11} &= U_{N-1}(z) [z + i\alpha_{ac}\zeta - i\beta_{ac}\beta_{ab} \cos(k_a a) \sin(k_b b)] - U_{N-2}(z) \\
m_{12} &= -U_{N-1}(z) [\beta_{ab} \sin(k_b b) (\sin(k_a a) + i\alpha_{ac} \cos(k_a a)) - i\beta_{ac}\zeta] \\
m_{21} &= -U_{N-1}(z) [\beta_{ab} \sin(k_b b) (\sin(k_a a) - i\alpha_{ac} \cos(k_a a)) + i\beta_{ac}\zeta] \\
m_{22} &= U_{N-1}(z) [z - i\alpha_{ac}\zeta + i\beta_{ac}\beta_{ab} \cos(k_a a) \sin(k_b b)] - U_{N-2}(z)
\end{aligned} \tag{13}$$

where,

$$\zeta = \sin(k_a a) \cos(k_b b) + \alpha_{ba} \cos(k_a a) \sin(k_b b), \tag{14}$$

The results (13) can then be combined to give the desired reflection and transmission coefficients. The transmissivity is found to be equal for incidence from the left and right,

$$T_+ = \left| \frac{1}{U_{N-1}(z) [z - i\alpha_{ac}\zeta + i\beta_{ac}\beta_{ab} \cos(k_a a) \sin(k_b b)] - U_{N-2}(z)} \right|^2 = T_- \tag{15}$$

Meanwhile the reflectivity is not,

$$\begin{aligned}
R_+ &= \left| \frac{U_{N-1}(z) [\beta_{ab} \sin(k_b b) (\sin(k_a a) - i\alpha_{ac} \cos(k_a a)) + i\beta_{ac}\zeta]}{U_{N-1}(z) [z - i\alpha_{ac}\zeta + i\beta_{ac}\beta_{ab} \cos(k_a a) \sin(k_b b)] - U_{N-2}(z)} \right|^2 \\
R_- &= \left| \frac{U_{N-1}(z) [\beta_{ab} \sin(k_b b) (\sin(k_a a) + i\alpha_{ac} \cos(k_a a)) - i\beta_{ac}\zeta]}{U_{N-1}(z) [z - i\alpha_{ac}\zeta + i\beta_{ac}\beta_{ab} \cos(k_a a) \sin(k_b b)] - U_{N-2}(z)} \right|^2
\end{aligned} \tag{16}$$

unless the medium is lossless, in which case it is evident that  $m_{12} = m_{21}^*$ . The reason for this difference is that, when incident from the left, light enters the medium initially into a region of index equal to  $n_a$ , and initially into a region of index equal to  $n_b$  when incident from the right. For thin layers with small dissipation, the difference is negligible. The expressions for  $R_+$  and  $T_+$  are plotted in figure 4, for a multilayer of 10 unit cells.

### A. An optical Bloch theorem

Any real multilayer system will have a finite number of layers; a Bragg reflector may only have tens or hundreds. It is therefore perhaps surprising that we can glean some of the behaviour illustrated in the previous section—culminating in figure 4—from the case of an infinite number of layers. Nevertheless, Bloch's theorem can be used to accurately predict the region of high reflectivity in the central region of figure 4 (20 layers). The reason for its applicability is that for such a range of frequencies, the wave is rapidly extinguished from

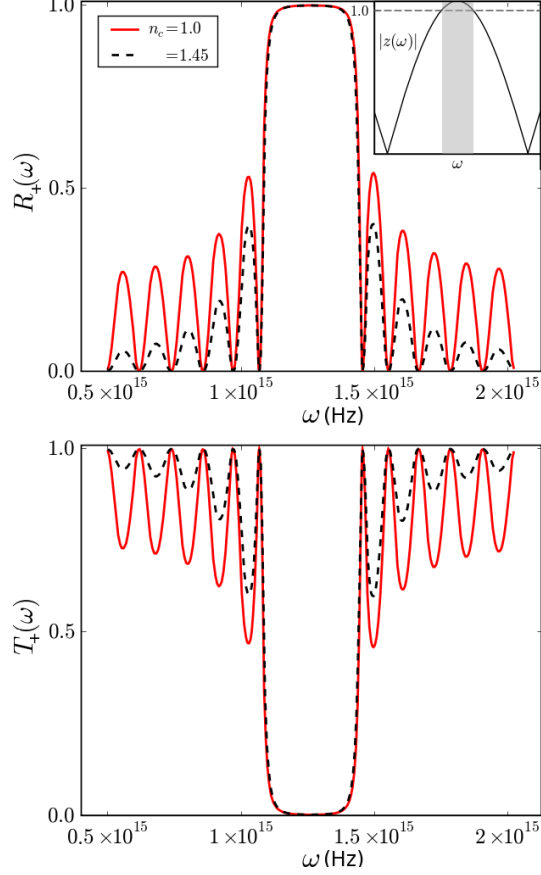


FIG. 4: Transmissivity  $T_+(\omega)$  and reflectivity  $R_+(\omega)$  as a function of frequency for a *transparent* Bragg reflector (photonic crystal). The system is composed of 10 unit cells where all layers have a real refractive index,  $n_a = 1.45$  and  $n_b = 2.1$ . The thicknesses of the layers are  $a = 2.60 \times 10^{-7}$  m and  $b = 1.76 \times 10^{-7}$  m. The spectra contain a stop-band region where propagation is forbidden, corresponding to the plateau in the central region of  $R_+$ , or to the grey shaded region where  $|z| > 1$  (inset). The amplitude of the oscillations increases with the index contrast from  $n_c = 1 \rightarrow n_c = 1.45$  at the edge of the crystal, but this does not affect the stop band structure. Such an increase in oscillation amplitude can be important (see section IV). *Inset*: For an infinite array of unit cells no mode can propagate in the frequency range shaded in grey ( $|z| > 1$ , corresponding to the photonic band gap).

the Bragg reflector so that the field amplitude is very close to zero at the exit interface, and we can consider the number of unit cells to be infinite with little error.

In an optical system with translational symmetry along an axis,  $x$ , the eigenstates,  $\mathbf{E}$

transform as  $\mathbf{E}(x + \delta) = \mathbf{E}(x)e^{ik\delta}$ , due to the fact that the translation operator commutes with the operators within the electromagnetic wave equation. Bloch's theorem is the analogue of this relation for the case when we do not have continuous translational symmetry, but instead an infinite periodic structure, with discrete translational symmetry. In this case, if the spatial periodicity is  $a + b$ , then the eigenmodes obey,

$$\mathbf{E}(x + a + b) = \mathbf{E}(x)e^{i\kappa(a+b)} \quad (17)$$

The quantity,  $\kappa$  is known as the Bloch wave-vector (see figure 3 for illustration). In general  $\kappa$  is complex, and designates a normal mode for light waves that propagate by coupling to the periodic medium. The Bloch wave-vector is the analogue of the free space wave-vector for the case of a discrete translational symmetry, and tells us the large scale variation of the field as one moves across one or more unit cells. In terms of the transfer matrix formalism outlined in the previous two sections, this statement is,

$$\mathcal{M}_1 \cdot \mathbf{e} = e^{i\kappa(a+b)} \mathbf{e}, \quad (18)$$

Equation (18) can be seen as analogous to the electronic Bloch theorem, where the unit cell transfer matrix,  $\mathcal{M}_1$  is playing the role of the translation operator, and the electric field  $\mathbf{e}$  is cast as the wave-function. Finding the relation between the frequency,  $\omega$ , and the Bloch-vector,  $\kappa$  amounts to finding the eigenvalues,  $\lambda = e^{i\kappa(a+b)}$  of the unit-cell matrix,  $\mathcal{M}_1$ . These eigenvalues can be found in the usual manner, taking the right hand side of (18) to the left and setting the determinant of the resulting matrix to zero,

$$\det(\mathcal{M}_1 - \lambda \mathbf{1}_2) = \begin{vmatrix} \mathcal{M}_{11} - \lambda & \mathcal{M}_{12} \\ \mathcal{M}_{21} & \mathcal{M}_{22} - \lambda \end{vmatrix} = 0,$$

or,

$$\lambda^2 - \lambda(\mathcal{M}_{11} + \mathcal{M}_{22}) + (\mathcal{M}_{11}\mathcal{M}_{22} - \mathcal{M}_{12}\mathcal{M}_{21}) = \lambda^2 - 2z\lambda + 1 = 0, \quad (19)$$

where we have used the fact that  $\det[\mathcal{M}_1] = 1$ . The quadratic equation on the right of (19) has the two solutions,

$$\lambda = z \pm \sqrt{z^2 - 1} = e^{i\kappa(a+b)} \quad (20)$$

These solutions determine the dispersion of the Bloch modes, *i.e.*, the function  $\kappa(\omega)$ . It can be seen directly from (9) that  $z = \text{Tr}[\mathcal{M}_1]/2$  is real for media with *real* refractive indices  $n_a$

and  $n_b$ . In this case the criterion for allowed propagation through the multilayer becomes quite simple, for when  $z \leq 1$  we have,

$$e^{i\kappa(a+b)} = z \pm i\sqrt{1-z^2}$$

which can be satisfied with a real Bloch wave-vector:  $\kappa = \pm \arccos(z)/(a+b)$ . Meanwhile, when  $z > 1$ , the right hand side of (20) is real, with one root greater, and one less than unity. This leads to a complex value of  $\kappa$ . Such solutions have divergent behaviour at infinity, and are therefore not allowed modes of the truly infinite system. The frequency intervals where  $z > 1$  correspond to the forbidden gaps where the real part of  $\kappa$  is restricted to be either 0 (for gaps opening at the centre of the Brillouin zone) or  $\pm\pi/(a+b)$  (opening at the Brillouin zone boundaries). While the former solutions with real  $\kappa$  describe light waves that propagate in the medium, the latter ones with complex  $\kappa$  can be interpreted as surface excitations (*Tamm states*). In a bounded medium these are evanescent waves that undergo *extinction* inside the medium in the direction normal to the boundary. The decay is due to strong Bragg reflections, a reversible process that does not lead to a loss of energy from the field, making reflection within the gap strictly unity.

In a *dissipative* periodic medium the situation becomes rather intricate:  $z$  is complex. To see how this modifies the situation, consider the case where a small degree of dissipation is present:  $z = \cos(\varphi) + i\eta$ , where both  $\varphi$  and  $\eta$  are real, and where  $\eta \ll 1$ . To first order in  $\eta$ ,

$$e^{i\kappa(a+b)} \sim \left(1 \pm \frac{\eta}{\sin(\varphi)}\right) e^{\pm i\varphi} \quad (21)$$

The presence of dissipation shifts the modulus of (21) away from unity. Therefore  $\kappa$  is in general complex when dissipation is present, even for modes falling within an allowed band. This has the simple interpretation that in an absorbing periodic medium, the propagation of Bloch waves is damped. This is a dissipative process, which prevents reflection from being unity. It is also clear that the forbidden gaps are significantly modified (see figure 6a). When the real part of  $\kappa$  is close to 0 or  $\pi/(a+b)$ —where the forbidden band would begin in the absence of dissipation—then  $\sin(\varphi) \sim 0$ , and the right hand side of (21) has a modulus significantly different from unity. Hence the distinction between allowed and forbidden bands becomes blurred (see section IV A). For large degrees of dissipation the band-gap may even disappear.

## IV. SOME EXAMPLE APPLICATIONS

So far the discussion may have been rather familiar. Although we have given a treatment of the Bragg reflector in terms of transfer matrices, which might not be the standard presentation for undergraduates, the formulae are mostly well-known. We shall now demonstrate how we may use these results to discuss some examples that are relevant to contemporary experimental set ups.

### A. A Bragg reflector of cold atoms loaded into an optical lattice

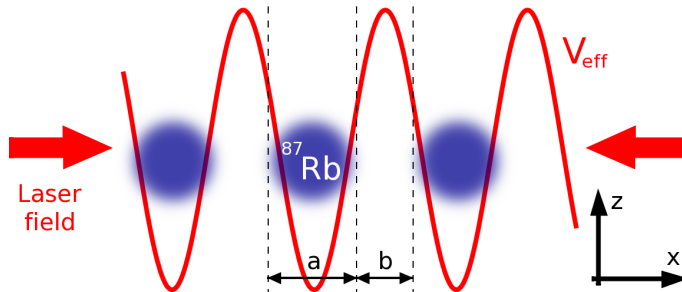


FIG. 5: Neutral atoms can be trapped within the electric field of two counter-propagating red-detuned laser beams. The electric field induces an atomic dipole moment, which interacts with the field, pushing the atomic centre of mass towards high field intensity. When sufficiently cooled these atoms can be trapped, and form a lattice. A weak probe beam interacts with the optical lattice in much the same way as the Bragg reflector illustrated in figure 3.

A neutral atom subject to an external electric field will develop an electric dipole moment,  $\mathbf{d}$ . The atom will then be subject to a force,  $\mathbf{F} = d\mathbf{p}/dt$ , due to interaction of the electromagnetic field with this induced polarization, and this force can be used to trap a cloud of such atoms within a confined region of space<sup>30</sup>. In the situation illustrated in figure 5, the interference pattern created by two counter-propagating laser fields creates an array of many thousand of such traps, often termed an *optical lattice*<sup>9</sup>. Once cold atoms are loaded into such a system then one has an array of interacting sites, each containing some average number of atoms per site, where the interaction strength of the atoms can be tuned via the laser field intensity. Within such a system one may create analogues of many body

phenomena in condensed matter physics<sup>31</sup>.

Consider a monochromatic field in which the induced atomic dipole moment can be written to first order in the electric field as,  $\mathbf{d} = \alpha(\omega)\mathbf{E}(\mathbf{r})$ , where  $\alpha(\omega)$  is the single-atom polarizability (assumed real and positive, as appropriate for a red detuned optical lattice),  $\mathbf{E}$  is the electric field amplitude (in this case a three dimensional vector), and  $\mathbf{r}$  is the position of the atomic centre of mass. The force on the centre of mass of each atom is, to first order in the size of the system,

$$\mathbf{F} = \frac{d\mathbf{p}}{dt} = \int [\rho\mathbf{E} + \mathbf{j} \times \mathbf{B}] dV \sim \int \mathbf{x}\rho(\mathbf{x} + \mathbf{r})dV \cdot \nabla_{\mathbf{r}}\mathbf{E}(\mathbf{r}) + \int \mathbf{j}(\mathbf{x} - \mathbf{r})dV \times \mathbf{B}(\mathbf{r})$$

where the integral is over the volume of the system of charges. We assume that the velocity of the centre of mass is slow enough that we can neglect contributions to the force of order  $\dot{\mathbf{r}}/c$ , and we also neglect the magnetic structure of the system. Identifying,  $\mathbf{d} = \int \mathbf{x}\rho(\mathbf{x} + \mathbf{r})dV$ , and  $\dot{\mathbf{d}} = \int \mathbf{j}(\mathbf{x} - \mathbf{r})dV$ <sup>57</sup>, the force on the centre of mass can be written as,  $d\mathbf{p}/dt = (\mathbf{d} \cdot \nabla_{\mathbf{r}})\mathbf{E}(\mathbf{r}) + \dot{\mathbf{d}} \times \mathbf{B}$ . For the particular case of an induced dipole moment this then becomes,

$$\frac{d\mathbf{p}}{dt} = \frac{1}{2}\alpha(\omega)\nabla|\mathbf{E}(\mathbf{r})|^2 + \alpha(\omega)\frac{\partial}{\partial t}(\mathbf{E} \times \mathbf{B}) \quad (22)$$

Figure 5 illustrates two counter-propagating optical beams that create the electric field that the atom encounters. Averaging the motion over a timescale significantly longer than the period of the optical field, the final term on the right (22) becomes negligible. The average force is then such that the atomic centre of mass will be pulled towards regions of high electric field intensity. In figure 5 the red line indicates the effective potential,  $V_{\text{eff}} = -\frac{1}{2}\alpha(\omega)|\mathbf{E}(\mathbf{r})|^2$ , in the minima of which we can imagine atoms collecting once their centre of mass motion has been cooled significantly by other means<sup>32</sup>.

Not only is the optical lattice useful as a model system, but it also has interesting optical properties of its own<sup>13,33</sup>. We can treat this system using the formalism developed in the previous sections (see figure 5). In the case of a one dimensional optical lattice, where the atomic motion is only weakly constrained in the  $y - z$  plane, the system is essentially a slightly unusual Bragg reflector (an ‘atomic Bragg mirror’). The reflector is approximately composed of layers of atomic clouds (width  $a$ , index  $n_a$ ), and layers of vacuum (width  $b$ ,  $n_b, n_c \sim 1$ ).

Suppose that a weak beam of light probes the atoms in the lattice; what are the reflection and transmission coefficients? When the frequency of this probe beam is close to an atomic

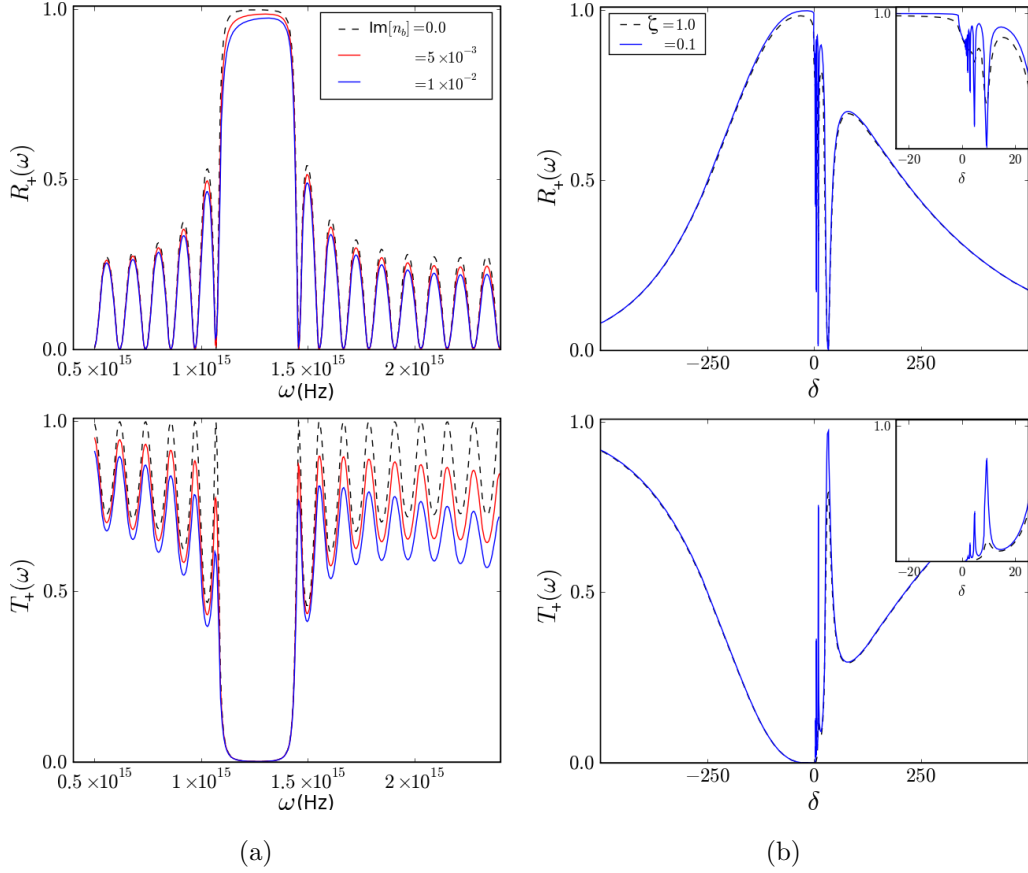


FIG. 6: Transmissivity  $T_+(\omega)$  and reflectivity  $R_+(\omega)$  as a function of frequency for a *dissipative* Bragg reflector. (a) The dissipative analogue of the plot shown in figure 4. All parameters are identical, but with the addition of an imaginary part to the refractive index,  $n_b$ . As  $\text{Im}[n_b]$  is increased, the contrast of the fringes around the stop band is decreased, and the shape of the reflectivity profile in the stop band changes. (b) The array of unit cells now describes the index profile of cold atoms trapped within an optical lattice ( $\mathcal{N} = 5.7 \times 10^{-3}$ ). The probe beam is assumed to be close to the frequency of the  $S_{1/2} \rightarrow P_{3/2}$  transition of  $^{87}\text{Rb}$ , where the index can be approximated by (23), with  $\omega_0 = 2.412 \times 10^{15}$  Hz,  $\gamma_e = 3.7699 \times 10^7$  Hz, and we use the notation,  $\delta = (\omega_0 - \omega)/\gamma_e$ . The trap has  $N = 5.4 \times 10^4$  periods, and the periodicity is such that  $a = 1.94807 \times 10^{-8}$  m, and  $b = 3.70873 \times 10^{-7}$  m. The blue and dashed lines illustrate the effect of changing the line shape parameter,  $\zeta$ .

resonance, the atom may be approximated as a two level system. The index of such a cloud of two-level atoms can then be calculated using the Maxwell-Bloch equations<sup>34</sup>, taking the

approximate form,

$$n_a(\omega) \approx \sqrt{1 + \frac{3\pi\mathcal{N}}{(\omega_0 - \omega)/\gamma_e - i\zeta}}. \quad (23)$$

In (23)  $\gamma_e$  is the linewidth of the excited state of the trapped atoms,  $\zeta$  is a parameter which modifies the shape of the resonance ( $\zeta = 1$  being the theoretical result emerging from the two-level approximation),  $\mathcal{N}$  is the scaled atomic density,  $A/(k_0^3V)$  ( $A/V$  atoms per unit volume), and  $k_0 = \omega_0/c$  is the resonant wave-vector associated with the frequency of atomic resonance,  $\omega_0$ .

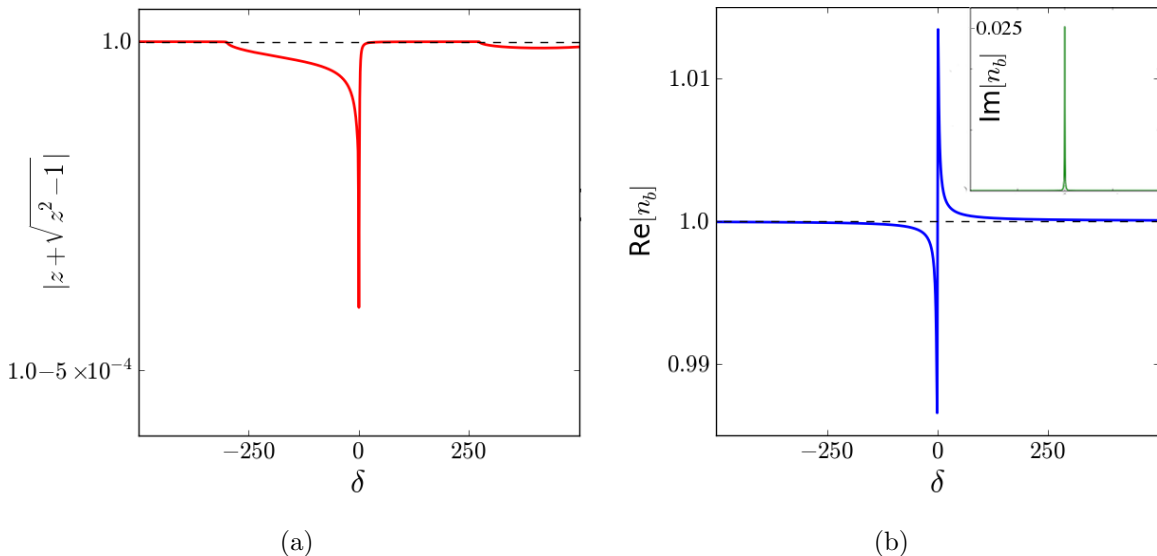


FIG. 7: (a) The absolute value of the right hand side of (20). The deviation of this quantity away from unity indicates the magnitude of the imaginary part of the Bloch wave-vector. (b) The real and imaginary (inset) parts of the refractive index computed from (23). In both cases the parameters and variables are as in figure 6b

Figure 6b shows the reflection and transmission coefficients calculated from (15–16), for the case of trapped  $^{87}\text{Rb}$ . We can see that close to the resonant frequency ( $\delta = 0$ ), where the dissipation and dispersion are both most pronounced, the optical response is quite complicated, with rapid oscillations evident on the scale of the  $\gamma_e$ . Either side of  $\delta = 0$  *two* bands of high reflectivity appear. Figure 7a is a plot of the absolute value of the right hand of (20), illustrating the origin of these two bands. For negative detuning away from resonance—where figure 6b shows nearly total reflection—the Bloch wave-vector has a significant imaginary part even though the absorption is small (inset of figure 7b). There

is also a stop band evident for positive detuning at around  $\delta \sim 250$ . This is not completely evident in figure 6b, where the reflectivity peaks at 0.6 for  $\delta \sim 150$ , but does become conspicuous for larger values of  $N$ .

This example system illustrates that when composed of resonant elements, the properties of the Bragg reflector can be quite subtle, and not at all like the textbook examples. Furthermore it shows that even when the layers have an index contrast of less than a percent away from unity, it is still possible to create an almost perfect reflector. This is so long as one can construct a system with  $N$  large enough, which is quite possible with an optical lattice<sup>35,36</sup>. These atomic Bragg mirrors can be devised to re-direct<sup>37</sup>, confine<sup>38</sup>, or amplify<sup>39</sup> radiation.

### B. Optomechanical cooling and heating

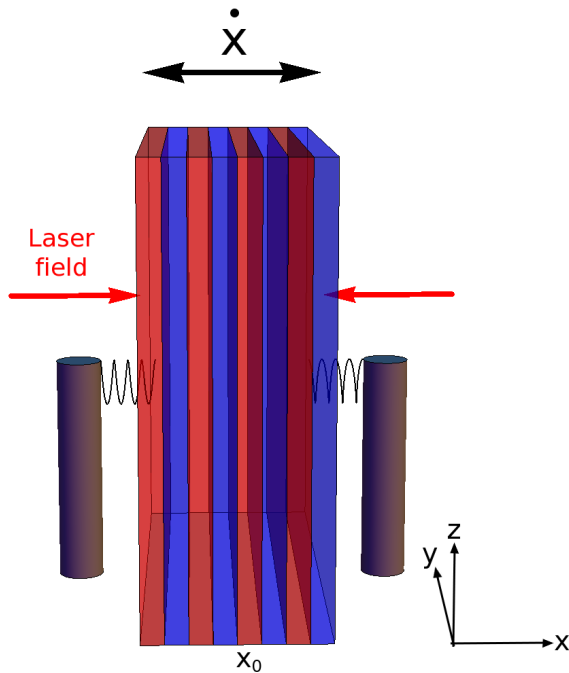


FIG. 8: A Bragg reflector is allowed to move along the  $x$  axis, confined by a pair of springs attached to fixed columns, and performing an oscillatory motion around the point  $x = x_0$ .

When equal amplitude, monochromatic light is incident onto both sides of the reflector, radiation pressure can be used to add or remove kinetic energy from the motion.

The electromagnetic field can add or remove energy from a mechanical degree of freedom. In much the same way that atomic motion can be cooled within an optical lattice, macroscopic mechanical motion can be reduced to the point where it enters regime where a quantum mechanical description must be used<sup>10,40</sup>. For example, in the case of a mechanical oscillator this would be when the total energy in the centre of mass motion becomes comparable with the spacing of the energy levels. Recent experimental work has succeeded in reducing the vibrational energy of macroscopic degrees of freedom to the quantum mechanical ground state<sup>41</sup>. We consider the system illustrated in figure 8 to demonstrate the basic principles (if not the detailed experimental set-up) involved in optomechanical cooling. This is inspired by the fact that a similar system has been recently proposed for this purpose<sup>33,42</sup>.

We imagine monochromatic radiation is incident onto both sides of a Bragg reflector, and due to the reflection from, and absorption into the body, it will exert a force. We calculate the optical force on the reflector by firstly examining the average balance of energy and momentum for the case of a single photon impinging on the structure at rest. In the rest frame of the reflector, we can use the reflection and transmission coefficients (15–16), where they are properly defined. For a photon incident from the left with momentum  $\hbar k_+ \hat{\mathbf{x}}$  and energy  $\hbar\omega_+$ , the difference in optical energy and momentum before and after interaction with the reflector would be found to be, on average,

$$\begin{aligned}\Delta E_+ &= \hbar\omega_+ [T_+(\omega_+) + R_+(\omega_+) - 1] \\ \Delta \mathbf{p}_+ &= \hbar k_+ [T_+(\omega_+) - R_+(\omega_+) - 1] \hat{\mathbf{x}}\end{aligned}\quad (24)$$

Similarly, for incidence from the right with momentum  $-\hbar k_- \hat{\mathbf{x}}$  and energy  $\hbar\omega_-$ ,

$$\begin{aligned}\Delta E_- &= \hbar\omega_- [T_-(\omega_-) + R_-(\omega_-) - 1] \\ \Delta \mathbf{p}_- &= -\hbar k_- [T_-(\omega_-) - R_-(\omega_-) - 1] \hat{\mathbf{x}}\end{aligned}\quad (25)$$

Assuming  $\mathcal{P}_\pm$  photons per second are incident from the left and right respectively, we can equate the rate of energy and momentum being lost from the field to that taken up by the medium. The rest frame force on the reflector is then,

$$\frac{d\mathbf{p}'_{\text{EM}}}{dt} = \hbar \{ \mathcal{P}_+ k_+ [1 + R(\omega_+) - T(\omega_+)] - \mathcal{P}_- k_- [1 + R(\omega_-) - T(\omega_-)] \} \hat{\mathbf{x}} \quad (26)$$

and the energy transfer (heating) is,

$$\frac{dE'_{\text{EM}}}{dt} = \hbar \{ \mathcal{P}_+ \omega_+ [1 - R(\omega_+) - T(\omega_+)] + \mathcal{P}_- \omega_- [1 - R(\omega_-) - T(\omega_-)] \} \quad (27)$$

assuming  $R_+ \sim R_- = R$  and  $T_+ = T_- = T$ .

Equal amplitude monochromatic radiation of frequency  $\omega$  incident onto both sides of the reflector is assumed in the laboratory frame. To first order in the velocity, the rest frame frequency and wave-vector are given in terms of laboratory quantities by,  $\omega_{\pm} = \omega(1 \mp \dot{x}/c) = ck_{\pm}$ . Furthermore, in the laboratory, the number of photons sent towards the medium per second,  $\mathcal{P}_0$  is equal on both sides of the reflector, and this also transforms as a frequency,  $\mathcal{P}_{\pm} = \mathcal{P}_0(1 \mp \dot{x}/c)$ . Expressions (26–27) are then,

$$\frac{d\mathbf{p}'_{\text{EM}}}{dt} = -\frac{2\hbar\omega\mathcal{P}_0}{c} \left(\frac{\dot{x}}{c}\right) \left\{ \omega \left[ \frac{\partial R(\omega)}{\partial \omega} - \frac{\partial T(\omega)}{\partial \omega} \right] + 2[1 + R(\omega) - T(\omega)] \right\} \hat{\mathbf{x}} \quad (28)$$

and,

$$\frac{dE'_{\text{EM}}}{dt} = 2\hbar\omega\mathcal{P}_0 [1 - R(\omega) - T(\omega)] \quad (29)$$

where the reflection and transmission coefficients have been expanded as, e.g.  $R(\omega_{\pm}) \sim R(\omega) \mp (\dot{x}\omega/c)\partial R(\omega)/\partial\omega$ . Finally, transforming (28–29) from the rest frame into the laboratory frame, using  $d\mathbf{p}_{\text{EM}}/dt \sim d\mathbf{p}'_{\text{EM}}/dt + (\dot{\mathbf{x}}/c^2)dE'_{\text{EM}}/dt$ , the optical force on the reflector due to the field is then of the form,

$$\frac{d\mathbf{p}_{\text{EM}}}{dt} = -\frac{2\hbar\omega\mathcal{P}_0}{c} \left(\frac{\dot{x}}{c}\right) \left\{ 1 + 3R(\omega) - T(\omega) + \omega \left[ \frac{\partial R(\omega)}{\partial \omega} - \frac{\partial T(\omega)}{\partial \omega} \right] \right\} \hat{\mathbf{x}} \quad (30)$$

Expression (30) is the optical contribution to the force on the medium, as observed in the laboratory frame. Defining the following quantity,

$$\Gamma = \frac{\hbar\omega\mathcal{P}_0}{c^2} \left\{ 1 + 3R(\omega) - T(\omega) + \omega \left[ \frac{\partial R(\omega)}{\partial \omega} - \frac{\partial T(\omega)}{\partial \omega} \right] \right\} \quad (31)$$

the equation of motion for the centre of mass of the Bragg reflector in the presence of the optical field becomes,

$$m\frac{d^2x}{dt^2} + 2\Gamma\frac{dx}{dt} + m\Omega^2(x - x_0) = 0 \quad (32)$$

where  $m$  is the mass of the reflector, and  $\Omega$  is the frequency associated with the restoring force of the springs (see figure 8). The equation of motion, (32) is of the form of a damped ( $\Gamma > 0$ ), or amplified ( $\Gamma < 0$ ) harmonic oscillator. The damping coefficient is proportional to the incident optical power, and depends on the reflection and transmission coefficients and their derivatives with respect to frequency. The solutions to (32) have the form,

$$x(t) = x_0 + A_0 e^{-\Gamma t/m} e^{\pm i\Omega\sqrt{1-\Gamma^2/m^2\Omega^2}t}$$

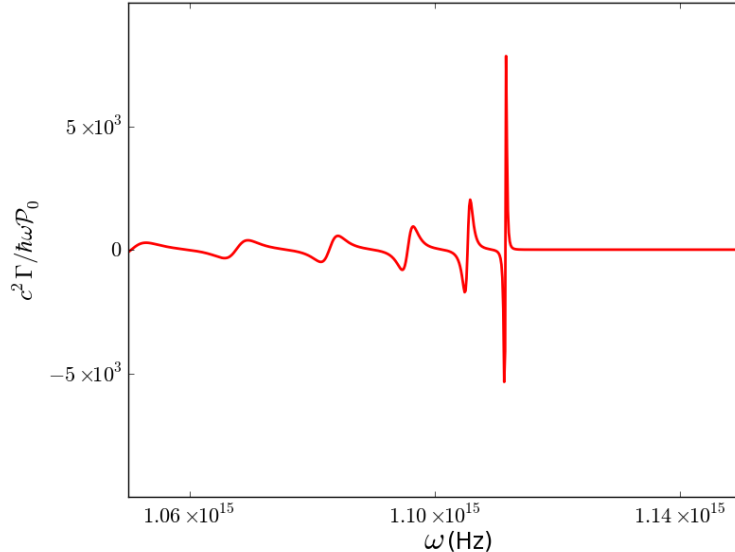


FIG. 9: The damping coefficient,  $\Gamma$  in units of  $\hbar\omega\mathcal{P}_0/c^2$ , for a Bragg reflector in a frequency regime around the edge of a stop band. The parameters are as in figure 4, but for the case of  $N = 50$  layers, where the stop band is more defined.

where  $A_0$  is the distance of the centre of mass from  $x_0$  at  $t = 0$ . If the medium is only weakly dispersive, then the derivatives of the reflection and transmission coefficients within (31) may be neglected: then  $\Gamma$  is strictly positive. Without such terms it is evident that the rate of damping is ordinarily very small. For instance, an optical field,  $\omega \sim 10^{15}$  Hz, and a reflector of a very small mass<sup>42</sup>,  $m \sim 10^{-15}$  kg, yields,  $\Gamma/m \sim 10^{-23}\mathcal{P}_0$ . For a moderate damping rate of  $\Gamma/m \sim 10^{-3}$  we would thus require  $\mathcal{P}_0 \sim 10^{20}$ , corresponding to a laser power per unit area of  $10 \text{ W}/\mathcal{A}$ , where  $\mathcal{A}$  is the cross sectional area of the reflector. In such a field the heating due to absorption alone would be enough to melt the medium.

Conversely for a Bragg reflector, dispersion is not negligible. Figure 4 shows there are strong oscillations in the reflection and transmission coefficients, contributing significantly to  $\Gamma$  via the frequency derivatives in (31). The motion can then be either amplified or damped, depending on the sign of the derivatives of the reflection and transmission coefficients. For small dissipation, and increasing reflectivity with frequency we have damping ( $\Gamma > 0$ ), while for decreasing reflectivity with frequency, we have amplification ( $\Gamma < 0$ ). Figure 9 illustrates  $c^2\Gamma/\hbar\omega\mathcal{P}_0$ , demonstrating four orders of magnitude increase in the absolute value of the damping coefficient. The required optical power density is correspondingly four orders of magnitude smaller. The above effect is the basic principle of optomechanical cooling.

It is worth mentioning that while the Bragg reflector is highly dispersive, a typical experiment in optomechanics involves an object that has relatively weak dispersion. However, the object sits within a high quality factor optical cavity. The frequency of incident radiation is close to a cavity resonance, which is the source of the strong dispersion in the equivalent of  $\Gamma^{58}$ .

### C. Optical non-reciprocity

Reciprocity—the fact that the same readings will be obtained when the positions of a source and detector of waves are interchanged—is a rather general property of wave propagation. For the purposes of performing signal processing, or computation with photons, one might like to realise an optical diode, allowing total light transmission in the forward direction, and inhibiting (over some bandwidth) propagation in the backward direction. Partly for this reason, current efforts are going into the realisation of non-reciprocal optical devices.

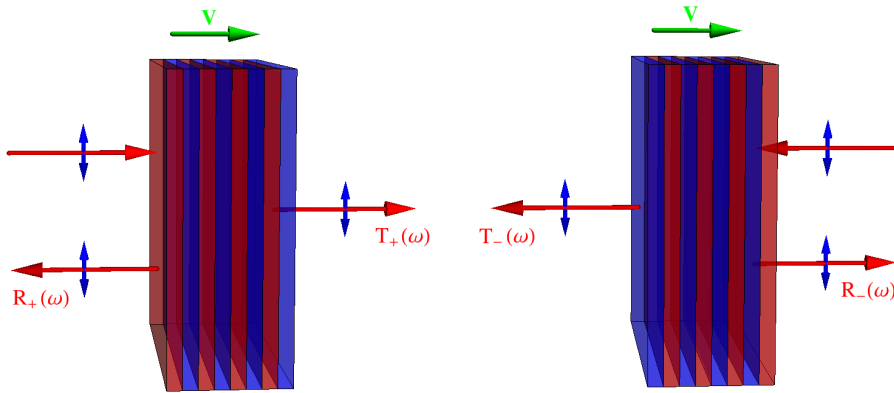


FIG. 10: In the laboratory frame a Bragg reflector moves with velocity  $\mathbf{v}$  along  $\hat{\mathbf{x}}$ . Light of frequency  $\omega$ , incident on the multilayer structure, is seen to exhibit significantly different reflection and transmission characteristics, depending on whether it impinges from the right  $\{R_-, T_-\}$ , or from the left  $\{R_+, T_+\}$ .

Non-reciprocal devices are often composed of materials exhibiting magneto-optical effects<sup>17,43</sup>, but these are difficult to integrate into an optical circuit. Nonlinear optics can also be used<sup>44,45</sup>, but good performance is then restricted to a specific power range. These two methods are by no means the only options, and for reference we note that several other

mechanisms for breaking reciprocity have been explored<sup>46–53</sup> some of which have been realized experimentally<sup>54</sup>. Here we illustrate the pervasiveness of electromagnetic reciprocity within the transfer matrix formalism of section II. A moving Bragg reflector provides a simple example of a system exhibiting significant non-reciprocity (due to the motion, which breaks time symmetry). Indeed close to the stop band edge its properties can be much like that of an optical diode.

Consider propagation through an arbitrary layered medium, as described in section II, and illustrated in figure 1. If the medium is reciprocal, then the transmission from the background index on the left of the medium to that on the right should be the same as transmission from right to left. We shall define a simple measure of the non-reciprocity of our layered medium to be,

$$\Delta T = T_+(\omega) - T_-(\omega). \quad (33)$$

where the transmission coefficients are those measured in the laboratory. This measure obviously doesn't capture everything that the full definition of non-reciprocity does (see e.g.<sup>17</sup>), but should be in qualitative agreement. Comparing (11) and (12) it is evident that reciprocity as defined by (33) requires  $\det[\mathbf{M}] = 1$ . For normal incidence onto a non-magnetic medium, an arbitrary transfer matrix is equal to a (possibly infinite) product of  $\mathbf{X}$  and  $\mathbf{W}$  matrices given by (3–4), and the determinant of such a product equals the product of the determinants,

$$\begin{aligned} \det[\mathbf{M}] &= \prod_{i=1}^N \det[\mathbf{X}^{(i)}(d_i)] \prod_{j=0}^N \det[\mathbf{W}^{(j,j+1)}] \\ &= \prod_{j=0}^N \frac{n_j}{n_{j+1}} = \frac{n_0}{n_{N+1}} \end{aligned} \quad (34)$$

where we have assumed an  $N$  layered medium, each layer having index  $n_i$  and thickness  $d_i$ . As defined here, (33) is applicable only to the case where  $n_0 = n_{N+1}$ , and thus  $T_+ = T_-$ . One may well ask about the case where we examine the electric field within the medium rather than outside, where the above analysis shows that  $\det[\mathbf{M}] \neq 1$ . Initially it appears that this case violates reciprocity. However this conclusion is incorrect, for the fundamental measure of reciprocity is about the field produced by a current of fixed amplitude, as registered by a detector. For cases where the source and detector are in different media, we must modify the simple measure (33).

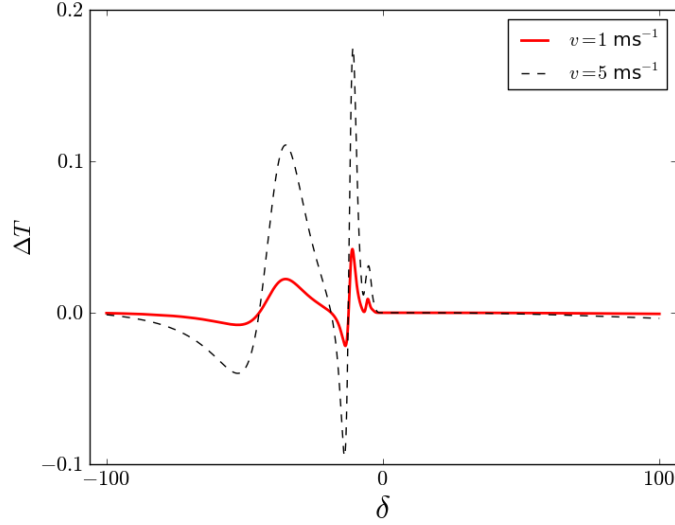


FIG. 11: Non reciprocal response, (33) for an atomic Bragg mirror set in motion. The velocity is  $1 \text{ ms}^{-1}$  (solid red) and  $5 \text{ ms}^{-1}$  (black dashed). The parameters are those given in figure 6b.

For the case illustrated above we have shown reciprocity to be necessarily embedded within the  $2 \times 2$  transfer matrix formalism. To break reciprocity we must do something to break this formalism. Perhaps the simplest way to do this is to take a medium that has been set into motion, as in figure 10. We cannot then simply imagine that  $\omega$  is the same throughout the system. Reflection causes the frequency of the waves to become  $\omega_{\pm} = \omega(1 \mp v/c)$ , and this will depend on the direction of incidence. Therefore, incident left and right going waves of frequency  $\omega$  will generate reflected and transmitted waves of frequencies,  $\omega_{\pm}$  and  $\omega$ : for two input channels we have four output channels. The  $2 \times 2$  formalism is therefore not applicable in the frame where the medium is in motion.

To calculate (33) for our system, we first examine propagation in the rest frame. For incidence from the left, the rest frame field on either side of the medium is

$$\mathbf{E}'(x') = \begin{cases} E_+ \hat{\mathbf{z}} [e^{i\omega_+ x'/c} + r_+(\omega_+) e^{-i\omega_+ x'/c}] & x' < 0 \\ E_+ \hat{\mathbf{z}} t(\omega_+) e^{i\omega_+ x'/c} & x' > L \end{cases} \quad (35)$$

and for incidence from the right,

$$\mathbf{E}'(x') = \begin{cases} E_- \hat{\mathbf{z}} t(\omega_-) e^{-i\omega_- x'/c} & x' < 0 \\ E_- \hat{\mathbf{z}} [e^{-i\omega_- x'/c} + r_-(\omega_-) e^{i\omega_- x'/c}] & x' > L \end{cases} \quad (36)$$

where the medium is taken to be of length  $L$ . Expressions (35–36) are transformed into the laboratory frame using the first order transformation,  $\mathbf{E} = \mathbf{E}' - \mathbf{v} \times \mathbf{B}'$ ,

$$\mathbf{E}(x) = \begin{cases} E_0 \hat{\mathbf{z}} [e^{i\omega x/c} + (1 - 2v/c)r_+(\omega_+)e^{-i\omega x/c}] & x < vt \\ E_0 \hat{\mathbf{z}} t(\omega_+)e^{i\omega x/c} & x > L + vt \end{cases} \quad (37)$$

and,

$$\mathbf{E}(x) = \begin{cases} E_0 \hat{\mathbf{z}}(1 + v/c)t(\omega_-)e^{-i\omega x/c} & x < vt \\ E_0 \hat{\mathbf{z}}(1 + v/c) [e^{-i\omega x/c} + (1 + 2v/c)r_-(\omega_-)e^{i\omega x/c}] & x > L + vt \end{cases} \quad (38)$$

where  $E_+ = E_0(1 - v/c)$  and  $E_- = E_0(1 + v/c)$ , the notation being as in section IV B. The difference in laboratory frame transmissivities for left and right incidence can thus be inferred from (37–38) and simply involves the difference in the rest frame transmission coefficients for two different Doppler shifted frequencies,

$$\Delta T = T_+ - T_- = |t(\omega(1 - v/c))|^2 - |t(\omega(1 + v/c))|^2 \quad (39)$$

To first order in the velocity of the medium, (39) is,

$$\Delta T \sim -\frac{2\omega v}{c} \frac{\partial T(\omega)}{\partial \omega} \quad (40)$$

where  $T(\omega)$  is the rest frame transmissivity. If dispersion is moderate then this measure of non-reciprocity is negligibly small for realistic velocities (say  $T$  changes 0.1 over  $10^{15}$  Hz then for optical frequencies and  $v \sim 1 \text{ ms}^{-1}$ ,  $\Delta T \sim 10^{-9}$ ). However, when the rest frame transmission coefficient depends strongly on frequency, then (39) may be large: again the Bragg reflector illustrates a prime example of this. Figure 11 gives a plot of  $\Delta T$  for an atomic Bragg mirror (section IV A) set into motion<sup>59</sup> at  $1 \text{ ms}^{-1}$  and  $5 \text{ ms}^{-1}$ . Due to the strongly dispersive optical response of the lattice (figure 6b) the non-reciprocity of this system as determined by  $\Delta T$  can be in the tens of percent for velocities of metres per second. For the same velocity regime, an effective optical diode exhibiting nearly 100% isolation would require only an order of magnitude increase in the dispersion. This could be realised in a three level systems driven by an optical field, as used to achieve electromagnetically induced transparency<sup>55,56</sup>.

## V. CONCLUSIONS

We have given an overview of the properties of the Bragg reflector using a simple application of the transfer matrix formalism. The basic physics of this system was found to be convenient for discussing several topical areas of optical physics. We used it, in particular, as the basis for a discussion of optomechanical cooling and optical nonreciprocity effects which can all be observed by using Bragg mirrors made of ultra-cold atoms.

### Acknowledgments

SARH thanks the EPSRC for financial support. This work is supported by the National Natural Science Foundation of China (11104112), the National Basic Research Program of China (2011CB921603), the CRUI-British Council Programs “Atoms and Nanostructures” and “Metamaterials”, and the IT09L244H5 Azione Integrata MIUR grant and the 2011 Fondo di Ateneo of Brescia University. Two of us (MA and GLR) would like to thank J.-H. Wu for the hospitality at Jilin.

---

\* Electronic address: s.horsley@exeter.ac.uk

- <sup>1</sup> M. Born and E. Wolf, *Principles of Optics* (Cambridge University Press, 1999).
- <sup>2</sup> D. Griffiths and N. Taussig, *Am. J. Phys.* **60**, 883 (1992).
- <sup>3</sup> D. J. Griffiths and C. A. Steinke, *Am. J. Phys.* **69**, 137 (2001).
- <sup>4</sup> W. Guo, *Am. J. Phys.* **74**, 595 (2006).
- <sup>5</sup> J. M. Ziman, *Principles of the theory of solids* (Cambridge University Press, Cambridge, UK, 1972).
- <sup>6</sup> E. M. Lifshitz and L. P. Pitaevskii, *Statistical Physics (Part 2)* (Butterworth-Heinemann, 2003).
- <sup>7</sup> R. J. Olsen and G. Vignale, *Am. J. Phys.* **78**, 954 (2010).
- <sup>8</sup> L. L. Sánchez-Soto, J. J. Monzón, A. G. Barriuso, and J. F. Cariñena, *Phys. Rep.* **513**, 191 (2012).
- <sup>9</sup> I. Bloch, *Nat. Phys.* **1**, 23 (2005).
- <sup>10</sup> F. Marquardt and S. M. Girvin, *Physics* **2**, 40 (2009).
- <sup>11</sup> R. J. Potton, *Rep. Prog. Phys.* **67**, 717 (2004).

- <sup>12</sup> D. Dai, J. Bauters, and J. E. Bowers, *Nat. Light Sci. & App.* **1**, e1 (2012).
- <sup>13</sup> M. Artoni, G. C. La Rocca, and F. Bassani, *Phys. Rev. E* **72**, 046604 (2005).
- <sup>14</sup> D. W. Berreman, *J. Opt. Soc. Am. A* **62**, 502 (1972).
- <sup>15</sup> M. Schubert, *Phys. Rev. B* **53**, 4265 (1996).
- <sup>16</sup> S. A. R. Horsley, M. Artoni, and G. C. La Rocca, *Phys. Rev. A* **86**, 053820 (2012).
- <sup>17</sup> L. D. Landau, E. M. Lifshitz, and L. P. Pitaevskii, *The Electrodynamics of Continuous Media* (Butterworth-Heinemann, Oxford, 2004).
- <sup>18</sup> J. W. S. Rayleigh, *Phil. Mag.* **26**, 256 (1887).
- <sup>19</sup> W. L. Bragg, *Proc. Cam. Phil. Soc.* **17**, 43 (1913).
- <sup>20</sup> T. F. Krauss, R. M. DeLaRue, and S. Brand, *Nature* **383**, 699 (1996).
- <sup>21</sup> S. Noda, K. Tomoda, N. Yamamoto, and A. Chutinan, *Science* **289**, 604 (2000).
- <sup>22</sup> E. Yablonovitch, *Phys. Rev. Lett.* **58**, 2059 (1987).
- <sup>23</sup> P. Lodahl, A. F. van Driel, I. S. Nikolaev, A. Irman, K. Overgaag, D. Vanmaekelbergh, and W. L. Vos, *Nature* **430**, 654 (2004).
- <sup>24</sup> S. John, *Phys. Rev. Lett.* **58**, 2486 (1987).
- <sup>25</sup> E. Cubukcu, K. Aydin, E. Ozbay, S. Foteinopoulou, and C. M. Soukoulis, *Nature* **423**, 604 (2003).
- <sup>26</sup> O. S. Heavens, *Rep. Prog. Phys.* **23**, 1 (1960).
- <sup>27</sup> P. Yeh, *Optical Waves in Layered Media* (Wiley, 2005).
- <sup>28</sup> I. S. Gradshteyn and I. M. Ryzhik, *Table of Integrals, Series and Products* (Academic Press, San Diego, USA, 2000).
- <sup>29</sup> C. Genet, A. Lambrecht, and S. Reynaud, *Phys. Rev. A* **67**, 043811 (2003).
- <sup>30</sup> R. Grimm, M. Weidemüller, and Y. B. Ovchinnikov, *Adv. At. Mol. Opt. Phys.* **42**, 95 (2000).
- <sup>31</sup> M. Lewenstein, A. Sanpera, and V. Ahufinger, *Adv. Phys.* **56**, 243 (2007).
- <sup>32</sup> F. Bardou, J.-P. Bouchaud, A. Aspect, and C. Cohen-Tannoudji, *Lévy Statistics and Laser Cooling: How Rare Events Bring Atoms to Rest* (Cambridge University Press, Cambridge, 2001).
- <sup>33</sup> S. A. R. Horsley, M. Artoni, and G. C. La Rocca, *Phys. Rev. Lett.* **107**, 043602 (2011).
- <sup>34</sup> J. Weiner and P.-T. Ho, *Light-Matter Interaction: Fundamentals and Applications (Volume 1)* (Wiley-Interscience, New Jersey, 2003).
- <sup>35</sup> A. Schilke, C. Zimmermann, P. W. Courteille, and W. Guerin, *Phys. Rev. Lett.* **106**, 223903

- (2011).
- <sup>36</sup> A. Schilke, C. Zimmermann, and W. Guerin, *Phys. Rev. A* **86**, 023809 (2012).
- <sup>37</sup> J.-H. Wu, Raczynski, J. Zaremba, S. Zielińska-Kaniasty, M. Artoni, and G. C. La Rocca, *J. Mod. Opt.* **56**, 768 (2009).
- <sup>38</sup> J.-H. Wu, M. Artoni, and G. C. La Rocca, *Phys. Rev. Lett.* **103**, 133601 (2009).
- <sup>39</sup> A. Schilke, C. Zimmermann, P. W. Courteille, and W. Guerin, *Nature Photonics* **6**, 101 (2012).
- <sup>40</sup> M. Aspelmeyer, S. Gröblacher, K. Hammerer, and N. Kiesel, *J. Opt. Soc. Am. B* **27**, A189 (2010).
- <sup>41</sup> J. Chan, T. P. Mayer Alegre, A. H. Safavi-Naeini, J. T. Hill, A. Krause, M. Gröblacher, S. ans Aspelmeyer, and O. Painter, *Nature* **478**, 89 (2011).
- <sup>42</sup> K. Karrai, I. Favero, and C. Metzger, *Phys. Rev. Lett.* **100**, 240801 (2008).
- <sup>43</sup> V. V. Konotop and V. Kuzmiak, *Physical Review B* **66**, 235208 (2002).
- <sup>44</sup> V. F. Nesterenko, C. Daraio, E. B. Herbold, and S. Jin, *Physical Review Letters* **95**, (2005).
- <sup>45</sup> O. Narayan and A. Dhar, *Europhysics Letters* **67**, 559 (2004).
- <sup>46</sup> L. Poladian, *Physical Review E* **54**, 2963 (1996).
- <sup>47</sup> M. W. Feise, I. V. Shadrivov, and Y. S. Kivshar, *Physical Review E* **71**, (2005).
- <sup>48</sup> A. Gevorgyan, A. Kocharian, and G. Vardanyan, *Optics Communications* **259**, 455 (2006).
- <sup>49</sup> I. Bitá and E. Thomas, *Journal of the Optical Society of America B-Optical Physics* **22**, 1199 (2005).
- <sup>50</sup> J. Winn, Y. Fink, and S. Fan, *Optics Letters* (1998).
- <sup>51</sup> M. Scalora, J. Dowling, C. Bowden, and M. Bloemer, *Journal of Applied Physics* **76**, 2023 (1994).
- <sup>52</sup> B. Liang, B. Yuan, and J.-C. Cheng, *Physical Review Letters* **103**, (2009).
- <sup>53</sup> Z. Yu, *Nature photonics* **3**, 91 (2009).
- <sup>54</sup> K. Gallo, G. Assanto, K. Parameswaran, and M. Fejer, *Applied Physics Letters* **79**, 314 (2001).
- <sup>55</sup> S. Harris, *Physics Today* **50**, 36 (1997).
- <sup>56</sup> M. Artoni and G. C. La Rocca, *Phys. Rev. Lett.* **96**, 073905 (2006).
- <sup>57</sup> This can be shown from the continuity equation. Multiply both sides by  $\mathbf{x} - \mathbf{r}$ , and integrate over the system,  $\int (\mathbf{x} - \mathbf{r}) \nabla_{\mathbf{x}} \cdot \mathbf{j} dV = - \int (\mathbf{x} - \mathbf{r}) \frac{\partial \rho}{\partial t} dV$ . Integrating the left hand side by parts, we have the result,  $\int \mathbf{j} dV = \int (\mathbf{x} - \mathbf{r}) \frac{\partial \rho}{\partial t} dV = \dot{\mathbf{d}}$ .
- <sup>58</sup> Furthermore, an important feature missing from the above analysis is the inclusion of the Shot

noise within the optical field. This extra fluctuation serves to counteract the cooling process.

<sup>59</sup> An atomic Bragg mirror may be set into motion by relatively detuning the two laser beams in figure 5 so that the interference pattern moves along at a velocity determined by the detuning. Alternatively the lattice may be given a sudden jolt so that the atoms slosh about within the wells. In this latter case the velocity of the medium is a periodic function of time.